Journal of Alloys and Compounds 509 (2011) L263–L266

Contents lists available at ScienceDirect

Journal of Alloys and Compounds

journal homepage: www.elsevier.com/locate/jallcom

Letter

Optical floating zone method growth and photoluminescence property of $MgNb_2O_6$ crystal

Liang Li[a], Guanlin Feng[a], Dejun Wang[b], Hang Yang[c], Zhongmin Gao[d], Benxian Li[d], Dapeng Xu[a,c,*], Zhanhui Ding[c], Xiaoyang Liu[d]

[a] State Key Laboratory of Superhard Materials, Jilin University, Changchun 130012, China
[b] College of Continuing Education, Changchun University, Changchun 130000, China
[c] College of Physics, Jilin University, Changchun 130012, China
[d] State Key Laboratory of Inorganic Synthesis and Preparative Chemistry, College of Chemistry, Jilin University, Changchun 130012, China

ARTICLE INFO

Article history:
Received 26 December 2010
Received in revised form 9 April 2011
Accepted 11 April 2011
Available online 20 April 2011

Keywords:
$MgNb_2O_6$
Crystal growth
X-ray diffraction
Luminescence

ABSTRACT

$MgNb_2O_6$ single crystals are grown by the optical floating zone method. The as-grown crystals are dark brown and have dimensions of Ø 4–6 mm × *L* 87 mm, with the largest crystal domain being Ø 5 mm × *L* 32 mm. After being annealed, the crystals fade to light brown. The powder X-ray diffraction analysis shows that the crystals have a columbite-type $MgNb_2O_6$ structure. The crystal grows along the *c*-axis and the cleavage plane is the (0 1 0) plane. Transmission polarized light microscopy measurements show that the crystal is free of low-angle grain boundaries and inclusions. The crystals have been characterized by Raman scattering, which reveals the change of Nb–O band in annealed and non-annealed samples. The photoluminescence spectra exhibit a broad and strong blue emission band centered at 435 nm.

1. Introduction

Binary niobate ceramics, with the formula $M^{2+}Nb_2O_6$ (where M^{2+} = Ca, Mg, or a transition metal) [1–10], have the orthorhombic columbite structure. Growing interest has been focused on the columbites as microwave dielectric ceramics because of their lower processing temperatures, less complicated processing, lower cost of niobium compared with tantalum and low-temperature co-fired ceramics (LTCC) temperatures with Cu^{2+} [11,12]. Recently, considerably more attention has been paid to the interesting magnetic properties of niobates [1].

As one of the best-known members of this group, $MgNb_2O_6$ exhibits excellent dielectric and optical properties. Moreover, it has been widely used as a precursor in the synthesis of single-phase PMN ($Pb(Mg_{1/3}Nb_{2/3})O_3$) [13–16]. $MgNb_2O_6$ melts congruently at about 1840 K. As early as 1968, $MgNb_2O_6$ crystals were grown by the chemical transport method [17,18] (size: 5 mm × 2 mm × 1 mm), and then by the flux method [19,20] in 1982 and 2004 (size: 5 mm × 4 mm × 3 mm and 2.7 mm × 5.1 mm × 1 mm). However, two problems persist in the above-mentioned methods: the size of the grown crystals is small and impurity is unavoidable. In 1995, Polgár et al. grew $MgNb_2O_6$ crystals using the Czochralski method [21], but impurities continued to be a problem because of the crucibles. Brück et al. grew $MgNb_2O_6$ crystal fiber using the laser-heated pedestal method [22], in which impurities were avoided; however, the grown crystal fiber had a small diameter (Ø <1 mm).

In contrast to the above-mentioned methods, the optical floating zone method is more suitable for growing high-quality single crystals because of the crucible-free condition, atmosphere-controllable environment and steep temperature gradients along the growth direction. Such conditions allow for more stable and faster crystal growth [23–28]. Furthermore, the size of the grown crystals by the optical floating zone method is usually suitable for experimental measurements [29–32]. To the best of our knowledge, no report on the growth of $MgNb_2O_6$ single crystals by the floating zone method has been published. In the current work, $MgNb_2O_6$ single crystal was grown by the optical floating zone method, and the photoluminescence property of the grown crystal was also investigated.

2. Experimental details

The starting $MgNb_2O_6$ polycrystalline powders were prepared by calcining stoichiometric amounts of MgO (Alfa Aesar 99.99%) and Nb_2O_5 (Alfa Aesar 99.99%) at 1500 K for 20 h with intermediate grinding. The $MgNb_2O_6$ powders were firstly packed into the cylindrical shape rubber tubes while evacuating air using a vacuum

* Corresponding author at: College of Physics, Jilin University, Jiefang Road 2519, Changchun 130012, Jilin Province, China. Tel.: +86 431 85167955; fax: +86 431 85167046.
E-mail address: xudp@jlu.edu.cn (D. Xu).

0925-8388/$ – see front matter © 2011 Elsevier B.V. All rights reserved.
doi:10.1016/j.jallcom.2011.04.063

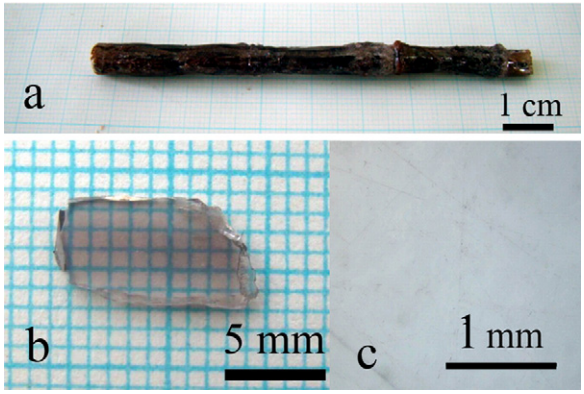

Fig. 1. Photographs of (a) an as-grown $MgNb_2O_6$ sample, (b) a wafer cut parallel to the growth direction and (c) the wafer under polarizing microscope in the transmission configuration.

pump, and then were pressed hydrostatically up to 70 MPa in a cold isostatic press to form the cylindrical rods of 4–6 mm in diameter and 100 mm in length. Finally, these rods were sintered in air at 1500 K for 10 h as the feed and support rods.

The crystals were grown using an optical floating zone furnace (CSI FZ-T-10000-H-VI-VP, Crystal Systems, Inc., Japan) which was equipped with four 1000 W halogen lamps as heat source. The growth conditions were as follows: the feed and support rods rotated in opposite directions at the rates of 30 rpm, respectively. The growth rate was 6 mm/h. The air flow at 0.1 L/min and the pressure of 0.1 MPa were applied.

The Raman spectra were taken with a Jobin-Yvon HR800 micro-Raman spectrometer with an argon laser at 514.5 nm as the light source. The macroscopic defects such as low-angle grain boundaries and inclusions were checked by Olympus Model BX-51 polarizing microscope in transmission configuration. The structure of the samples was characterized using a Rigaku D/max-r A 12 kW X-ray diffractometer (XRD) with Cu Kα radiation. A Bruker AXS D8 Discover with GADDS X-ray diffractometer (XRD^2) was used to probe the orientation of the as-grown crystal, in which a part of the Debye–Sherrer ring is two-dimensionally detected. As a result, orientation can be characterized easily. The photoluminescence spectra were measured by Jobin Yvon Fluoro Max-4 spectrophotometer equipped with xenon lamp.

3. Results and discussion

When a pure oxygen atmosphere was applied, many bubbles were observed in the melt, which resulted in an unstable molten zone. In the air atmosphere, no bubbles appeared and the molten zone was more stable. In addition, a higher lamp power resulted that more liquid could be replenished from the melting feed rod than that would be crystallized. The optimal experimental condition was the lamps power of 62.1% in the air flow of 0.1 L/min and the pressure of 0.1 MPa. $MgNb_2O_6$ crystals were grown by spontaneous nucleation. As growth began, multiple nucleation sites were observed. After optimization, the as-grown rod was composed of several large domains as shown in Fig. 1a. The as-grown crystal is a dark-brown cylindrical rod of 4–6 mm in diameter and 87 mm in length, with the largest crystal domain being Ø 5 mm × L 32 mm. The dark brown color in the as-grown crystal can be attributed to the partial reduction of Nb^{5+} ions, a common problem with alkali-earth niobates grown directly from their melts [20,22]. Fig. 1b shows a crystal wafer cut parallel to the growth direction, and then annealed in an oxygen atmosphere at 1500 K for 10 h. The color of the annealed wafer fades to light brown.

The powder XRD pattern of the as-grown crystal is shown in Fig. 2. All the peaks can be indexed to the diffraction peaks of the $MgNb_2O_6$ columbite (Ref: PDF Number: 330875), indicating that the as-grown crystal is columbite $MgNb_2O_6$ without any other phase. The powder XRD pattern of the annealed crystal was also measured; its peak positions and relative intensity are unchanged, indicating that the annealing has no effect on the crystal structure.

The room-temperature Raman spectra of the as-grown and annealed wafers are shown in Fig. 3a and b, respectively. The spectra present typical bands corresponding to the normal vibration

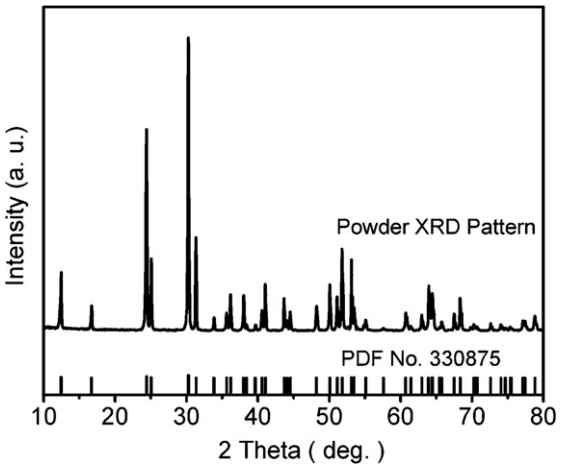

Fig. 2. Powder XRD pattern of the as-grown crystal.

modes of $MgNb_2O_6$ [33]. The maximum phonon model can be indexed to the Nb–O stretching band, and the linewidths (FWHM) for the line at 905 cm^{-1} of the as-grown and annealed wafers are fitted to be 8.2 and 6.8 cm^{-1}, as shown in the insets of Fig. 3a and b, respectively. For the as-grown crystal, the dark brown color can be attributed to the partial reduction of Nb^{5+} ions mainly originating from the NbO_6 octahedron [22,34]. The partial reduction of Nb^{5+} ions caused by the oxygen vacancies results in the change in the Nb–O stretching vibration, so that the band at 905 cm^{-1} is broadened. After being annealed, the oxygen vacancies in the as-grown crystal are eliminated; the Nb ions are the same Nb^{5+}; the band lengths of the Nb–O are more uniform. These result in a higher degree of order on the Nb and Mg sublattices [22]. Therefore, the linewidth at 905 cm^{-1} is narrowed and the annealed crystal fades to light brown. The annealing process eliminates the oxygen vacancies.

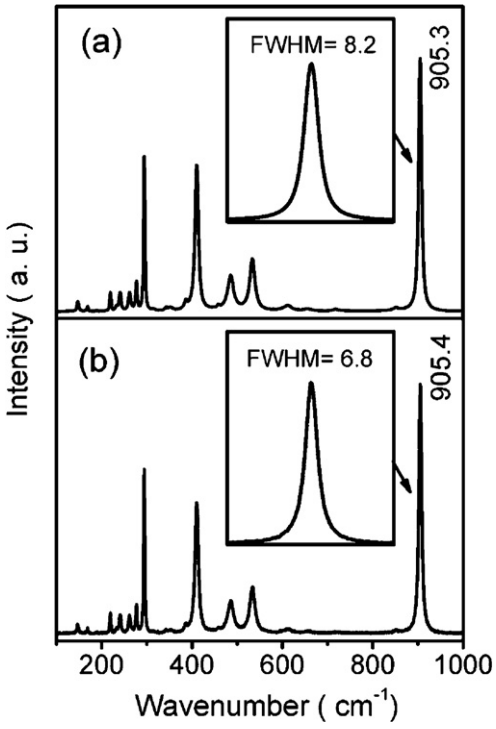

Fig. 3. (a) Raman spectrum of the as-grown crystal and the fitted peak at 905 cm^{-1} and (b) Raman spectrum of the annealed crystal and the fitted peak at 905 cm^{-1}.

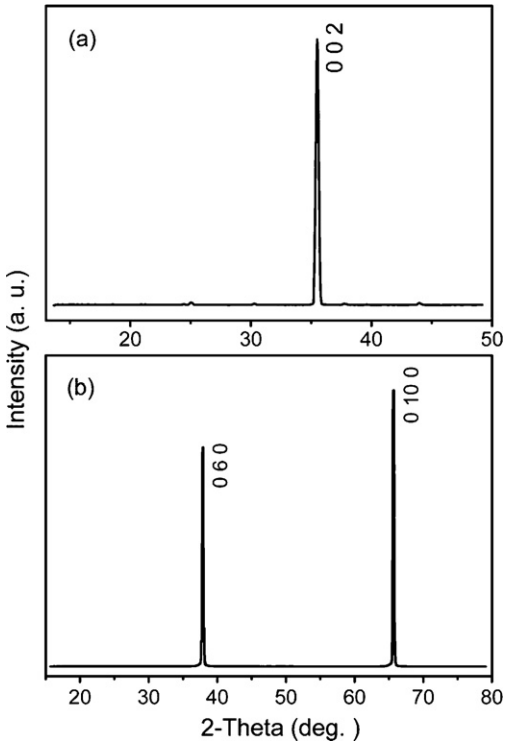

Fig. 4. XRD[2] patterns of (a) the cross-section perpendicular to the growth direction of the crystal and (b) the cleavage plane parallel to the growth direction of the crystal.

To determine the growth direction of $MgNb_2O_6$ single crystal, XRD[2] was conducted on the cross-section of the crystal, which was perpendicular to the growth direction (Fig. 4a). Only one peak locates at 35.35°, which can be indexed to the (0 0 2) plane. The natural cleavage plane parallel to the growth direction was also tested by XRD[2], as shown in Fig. 4b. Two peaks are found at 38.11° and 65.80°, which can be indexed to the (0 6 0) and (0 10 0) planes, respectively. These results indicate that the $MgNb_2O_6$ crystal cleaves along the (0 1 0) plane and the crystal grows along the *c*-axis. The XRD[2] and Raman results suggest that the annealed crystal is a single crystal of high perfection and crystallinity.

The macroscopic defects, such as the low-angle grain boundaries and inclusions of the crystal, were examined by polarized-light microscopy in the transmission configuration. Fig. 1c shows a photograph of the wafer (Fig. 1b) under polarized-light. Neither inclusions nor low-angle grain boundaries are observed on the wafer.

Fig. 5 presents the room-temperature photoluminescence spectra of both the as-grown and annealed wafers with excitation at 282 nm. A strong blue emission band centered at 435 nm can be observed in the two wafers. In the previous works, two peaks located at 420 and 485 nm were observed in the crystal fibers grown by the laser-heated pedestal growth method [22]; however, no detailed explanations were provided. Moreover, in the polycrystalline samples, an emission peak centered at 450 nm was reported, a finding that agrees with the results of the present study [6,35–37]. The luminescence in $MgNb_2O_6$ is strongly dependent on its crystal structure [36,38]. In the columbite structure, Mg and Nb cations are at the center of the octahedral surrounded by six oxygen atoms. The MgO_6 and NbO_6 octahedra form independent zig-zag chains by sharing edges, and the chains are connected by sharing corners in the order MgO_6 chain–NbO_6 chain–NbO_6 chain [39]. Here, the corner-shared NbO_6 groups are efficient luminescent centers for the blue emission [38], which may be ascribed to the recombination of self-trapped excitons. Between the

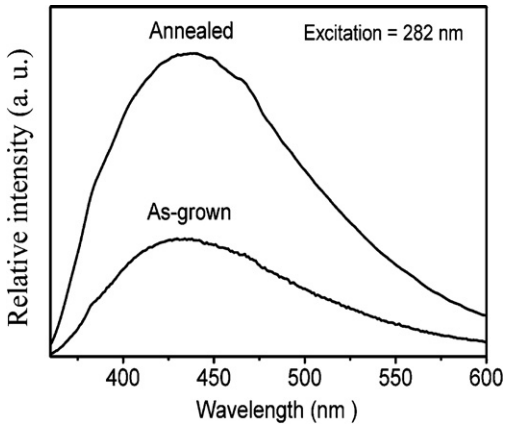

Fig. 5. Room-temperature photoluminescence spectra of the as-grown and annealed wafers.

corner-sharing NbO_6 octahedrals [37], the conduction band is composed of Nb^{5+} 4d orbitals and the valence band is composed of O^{2-} 2p orbitals. This luminescence originates from the absorbing groups of the niobate octahedral group $[NbO_6]^{7-}$. Thus, the low luminescence intensity is caused by the oxygen vacancies leading to the band length change in the NbO_6 octahedral, which should be similar as the broadening of the Raman band at 905 cm^{-1} (Fig. 3). After being annealed under an oxygen atmosphere, the oxygen vacancies in the crystal are eliminated. So the oxidation state of Nb ions are in the same Nb^{+5}, and the Nb and Mg sublattices are of higher degree of order, resulting in a more perfect structure of the NbO_6 octahedral. Therefore, the annealed wafer exhibits a stronger intensity than that does the as-grown sample, as shown in Fig. 5. Because the oxygen vacancies are eliminated; the improved crystallinity leads to higher oscillation strengths, which in turn results in the improvement in photoluminescence performance. These observations agree with the discussion about the Raman spectra and the color change of the crystal before and after being annealed [22].

4. Conclusions

By the optical floating zone method, the $MgNb_2O_6$ single crystals have been grown at a growth speed of 6 mm/h and a rotation rate of 30 rpm under an air atmosphere. The as-grown crystal has dimensions of Ø 4–6 mm × *L* 87 mm, with the largest crystal domain being Ø 5 mm × *L* 32 mm. The color of the as-grown crystal is dark brown and fades to light brown after annealing under an oxygen atmosphere. The single crystal grows along the *c*-axis and the natural cleavage plane is the (0 1 0) plane. The crystal is also free of low angle grain boundaries and inclusions. The photoluminescence spectra of the crystals have a strong blue emission band centered at 435 nm. The oxygen vacancies of the as-grown crystal can be eliminated by annealing process under an oxygen atmosphere, which results in the color change of the crystal, the narrowing of the FWHM of the Nb–O stretching band (905 cm^{-1}), and the increase in luminescence intensity.

Acknowledgements

Project 20101048 supported by Graduate Innovation Fund of Jilin University and Project 156 (2010) supported by Department of Education of Jilin Province are greatly appreciated.

References

[1] R. Coldea, D.A. Tennant, E.M. Wheeler, E. Wawrzynska, D. Prabhakaran, M. Telling, K. Habicht, P. Smeibidl, K. Kiefer, Science 327 (2010) 177–180.

[2] R.J. Sherlock, T.J. Glynn, G. Walker, G.F. Imbusch, K.W. Godfrey, J. Lumin. 72–74 (1997) 268–269.
[3] R.C. Pullar, K. Okeneme, N.M. Alford, J. Eur. Ceram. Soc. 23 (2003) 2479–2483.
[4] J.C. Brice, O.F. Hill, P.A.C. Whiffin, J.A. Wilkinson, J. Cryst. Growth 10 (1971) 133–138.
[5] R.C. Pullar, J. Am. Ceram. Soc. 92 (2009) 563–577.
[6] T.H. Fang, Y.J. Hsiao, Y.S. Chang, L.W. Ji, S.H. Kang, Curr.Opin. Solid State Mater. Sci. 12 (2008) 51–54.
[7] Y.J. Hsiao, Y.S. Chang, G.J. Chen, Y.H. Chang, J. Alloys Compd. 471 (2009) 259–262.
[8] Y.J. Hsiao, C.W. Liu, B.T. Dai, Y.H. Chang, J. Alloys Compd. 475 (2009) 698–701.
[9] L. Macalik, M. Maczka, J. Hanuza, P. Godlewska, P. Solarz, W. Ryba-Romanowski, A.A. Kaminskii, J. Alloys Compd. 451 (2008) 232–235.
[10] R.L. Moreira, N.G. Teixeira, M.R.B. Andreeta, A.C. Hernandes, A. Dias, Cryst. Growth Des. 10 (2010) 1569–1573.
[11] R. Pasricha, V. Ravi, Mater. Lett. 59 (2005) 2146–2148.
[12] Y.-C. Liou, Y.-T. Chen, W.-C. Tsai, J. Alloys Compd. 477 (2009) 537–542.
[13] S.A. Markgraf, A.S. Bhalla, Mater. Lett. 28 (1996) 221–224.
[14] D.a. Liu, Y. Zhang, W. Wang, B. Ren, Q. Zhang, J. Jiao, X. Zhao, H. Luo, J. Alloys Compd. 506 (2010) 428–433.
[15] X. Chao, D. Ma, R. Gu, Z. Yang, J. Alloys Compd. 491 (2010) 698–702.
[16] Y. Lin, B. Ren, X. Zhao, D. Zhou, J. Chen, X. Li, H. Xu, D. Lin, H. Luo, J. Alloys Compd. 507 (2010) 425–428.
[17] F. Emmenegger, A. Petermann, J. Cryst. Growth 2 (1968) 33–39.
[18] F. Emmenegger, J. Cryst. Growth 3–4 (1968) 135–140.
[19] M. Greenblatt, B.M. Wanklyn, B.J. Garrard, J. Cryst. Growth 58 (1982) 463–466.
[20] S. Oishi, Y. Kawatani, T. Suzuki, N. Ishizawa, J. Mater. Sci. 39 (2004) 1467–1469.
[21] K. Polgár, A. Péter, J. Paitz, C. Zaldo, J. Cryst. Growth 151 (1995) 365–368.
[22] E. Brück, R.K. Route, R.J. Raymakers, R.S. Feigelson, J. Cryst. Growth 128 (1993) 842–845.
[23] J.D. Pless, N. Erdman, D. Ko, L.D. Marks, P.C. Stair, K.R. Poeppelmeier, Cryst. Growth Des. 3 (2003) 615–619.
[24] A. Majchrowski, M. Swirkowicz, L. Jaroszewicz, M. Piasecki, I.V. Kityk, M.G. Brik, Mater. Lett. 64 (2010) 2363–2365.
[25] S. Otani, T. Aizawa, J. Alloys Compd. 454 (2008) 147–149.
[26] D. Prabhakaran, F.R. Wondre, A.T. Boothroyd, J. Cryst. Growth 250 (2003) 72–76.
[27] L. Li, H. Yang, D. Wang, G. Feng, B. Li, Z. Gao, D. Xu, Z. Ding, X. Liu, J. Cryst. Growth 312 (2010) 3561–3563.
[28] A.T.M.N. Islam, O. Pieper, B. Lake, K. Siemensmeyer, Cryst. Growth Des. 11 (2010) 154–157.
[29] P. Yu, A. Wu, L. Su, X. Guo, Y. Wang, H. Zhao, Y. Yang, Q. Yang, J. Xu, J. Alloys Compd. 503 (2010) 380–383.
[30] H. Feng, D. Ding, H. Li, S. Lu, S. Pan, X. Chen, G. Ren, J. Alloys Compd. 489 (2010) 645–649.
[31] M.H. Phan, V. Franco, N.S. Bingham, H. Srikanth, N.H. Hur, S.C. Yu, J. Alloys Compd. 508 (2010) 238–244.
[32] A. Rudajevová, J. Pospísil, J. Alloys Compd. 509 (2011) 5500–5505.
[33] E. Husson, Y. Repelin, N.Q. Dao, H. Brusset, J. Chem. Phys. 67 (1977) 1157–1163.
[34] R. de Almeida Silva, A.S.S. de Camargo, C. Cusatis, L.A.O. Nunes, J.P. Andreeta, J. Cryst. Growth 262 (2004) 246–250.
[35] A. Wachtel, J. Electrochem. Soc. 111 (1964) 534–538.
[36] Y. Zhou, Z. Qiu, M. Lü, Q. Ma, A. Zhang, G. Zhou, H. Zhang, Z. Yang, J. Phys. Chem. C 111 (2007) 10190–10193.
[37] A.M. Srivastava, J.F. Ackerman, W.W. Beers, J. Solid State Chem. 134 (1997) 187–191.
[38] G. Blasse, Struct. Bond. 42 (1980) 1–41.
[39] M. Maeda, T. Yamamura, T. Ikeda, Jpn. J. Appl. Phys. 26 (2) (1987) 76–79.